

1

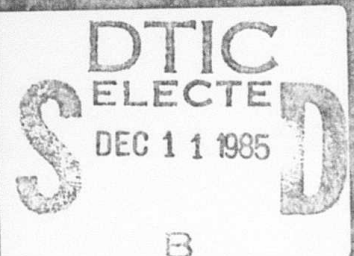
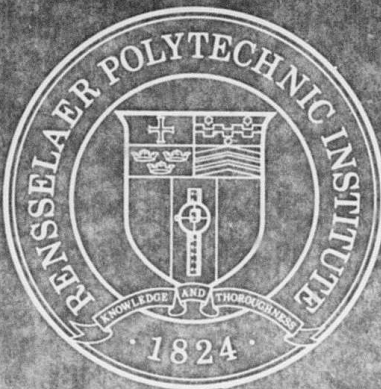
A LASER TRIANGULATION  
RANGING SYSTEM FOR  
MOBILE ROBOTS

by

Albert Lester Hoogeveen

AD-A162 846

100% COPY



Rensselaer Polytechnic Institute  
Troy, New York 12181

DISTRIBUTION STATEMENT A

Approved for public release  
Distribution Unlimited

85 12 10 024

(1)

RPI TECHNICAL REPORT MP-81

A LASER TRIANGULATION  
RANGING SYSTEM FOR  
MOBILE ROBOTS

by

Albert Lester Hoogeveen

Contract MDA-903-82-K-0168

DARPA Order no. 4467

DTIC  
ELECTE  
S D  
DEC 11 1985  
B

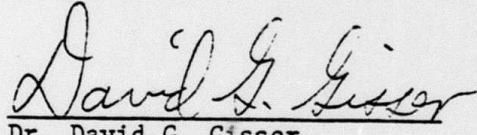
APPROVED FOR PUBLIC RELEASE  
DISTRIBUTION IS UNLIMITED (A)

School of Engineering  
Rensselaer Polytechnic Institute  
Troy, New York

May 1983

A LASER TRIANGULATION RANGING SYSTEM  
FOR MOBILE ROBOTS  
by  
Albert Lester Hoogeveen  
A Project Submitted to the Graduate  
Faculty of Rensselaer Polytechnic Institute  
in Partial Fulfillment of the  
Requirements for the Degree of  
MASTER OF ENGINEERING

Approved:



Dr. David G. Gisser  
Project Advisor



Rensselaer Polytechnic Institute  
Troy, New York

May 1983

Accession For	
NTIS GRA&I <input checked="" type="checkbox"/>	
DTIC TAB <input type="checkbox"/>	
Unannounced <input type="checkbox"/>	
Justification <i>Letter of file</i>	
By _____	
Distribution/ _____	
Availability Codes	
Dist	Avail and/or Special
A-1	

## CONTENTS

	Page
LIST OF FIGURES.....	iv
ACKNOWLEDGEMENT.....	v
ABSTRACT.....	vi
1. INTRODUCTION.....	1
1.1 Background.....	1
1.2 The Multi-Laser, Multi-Detector System.....	4
1.3 The Adaptive Suspension Vehicle.....	6
2. A NEW MULTI-LASER, MULTI-DETECTOR SYSTEM.....	8
2.1 Scanner Description.....	8
2.2 Scan Pattern.....	9
2.3 Theoretical Resolution.....	10
2.4 Control Electronics.....	11
3. LASER DEFLECTION TECHNIQUES.....	20
3.1 Mechanical Deflectors.....	20
3.2 Electro-optics.....	22
3.3 Diffraction.....	24
3.3.1 Acousto-optics.....	25
3.3.2 Holographics.....	27
4. HOLOGRAPHIC DIFFRACTION GRATINGS.....	29
4.1 Classification of Holograms.....	29
4.1.1 Thick Films vs. Thin Films.....	29
4.1.2 Phase and Amplitude Modulation.....	31
4.2 Dichromated Gelatin Films.....	32
4.2.1 Mechanism of Hologram Formation.....	32
4.2.2 Diffraction Efficiency.....	34
4.3 IDC's Holographic Scanner.....	35

	Page
5. SOURCES AND RECEIVERS.....	36
5.1 Laser Diodes.....	36
5.2 Photodiode Detectors.....	38
5.3 Optics.....	41
6. CONCLUSIONS.....	44
7. REFERENCES.....	48

## LIST OF FIGURES

	Page
Figure 1. Triangulation Equations.....	5
Figure 2. Triangulation Uncertainty.....	12
Figure 3. Electronics Block Diagram.....	14
Figure 4. Programmable Timing Module Outputs.....	15
Figure 5. Programmable Timing Module and Detector Latches....	16
Figure 6. High Order Detection.....	17
Figure 7. Low Order Detection.....	19
Figure 8. Electro-optic Deflector.....	23
Figure 9. Lenses and Equations.....	43

#### ACKNOWLEDGEMENT

The author wishes to express his sincere gratitude to Dr. David G. Gisser for the guidance and encouragement received under his supervision, and Dr. Steven Yerazunis for his unbelievable drive and dedication to this project; his enthusiasm for life is an inspiration to all around him.

Special thanks are extended to Dexter Smith and Tom Clement for their day to day support. Finally, the author is especially grateful to Barb for her patience and support over the past five years.

## ABSTRACT

A laser triangulation system for short range obstacle avoidance for mobile robots is discussed. The system was designed as an improvement over a laser triangulation system developed at Rensselaer Polytechnic Institute over the past 14 years. The new system was designed for use with an Adaptive Suspension Vehicle and the Mars Roving Vehicle; however, the new system is not limited to these two applications. A system overview is given, and then each component is discussed in detail.

## PART 1

### INTRODUCTION

The thought of robots has intrigued man for probably hundreds of years, but not until the Industrial Revolution did people begin to turn some of their mental and physical abilities over to machines. Out of these earliest mechanical contraptions, poets, writers, and scientists created a fantasy which is just now becoming a reality. The mechanization of laborious physical and mental tasks of industrial and commercial life is coming about through the advancement of intelligent machines.

#### 1.1 Background

As the complexity of robots and their tasks increase, sensory capability becomes more and more important. Mobile robots are especially dependent upon vision systems to allow any reasonable freedom of movement in changing environments. A fast and accurate vision system along with artificial intelligence can provide a mobile robot with the capability of autonomous navigation in various environments and terrains.

The Mars Rover Project at Rensselaer Polytechnic Institute has been dedicated to the development of an autonomous roving vehicle with a fast and accurate obstacle detection system. Originally the project focused on the design of a planetary vehicle under a NASA grant in 1968. Studies included steering, propulsion, payload, and suspension for a roving vehicle. Ten years later the Rover, as it is

affectionately called, had evolved into its present state, using on board microprocessor control and four wheel independent drive.

During the past five years, studies have been directed towards an obstacle detection system. The round trip communications delay time (9-40 minutes) between earth and the planet Mars, the Rover's original destination, made realtime earth control unfeasible. The Rover had to be able to travel to specific locations selected by NASA as fast as 1.5 meters/minute. This necessitated the change to an autonomous roving vehicle, capable of negotiating and maneuvering through rough, unknown terrain.

The human facility for extracting range information from visual cues is well documented in psychology texts. Human depth cues include texture gradient, size perspective, linear perspective, binocular perspective (eye control muscle feedback), motion perspective, aerial perspective, relative upward location in visual field, outline continuity, occlusion, and stereo disparity [1]. Three range finding methods in the area of mobile robots that have received the majority of attention include stereo disparity, time of flight, and triangulation-based methods.

Stereo disparity methods normally depend on two separate video cameras looking on a naturally lit scene. Stereo disparity requires sharp detail to operate effectively, is computationally expensive, and suffers from the "missing parts problem." It is computationally expensive in the sense that it takes a lot of computer power and time to receive and process data. In mobile robots where

real time processing is essential, stereo disparity has met with considerable difficulty. The "missing parts problem" comes from the fact that in certain terrains parts of the scene are not in both images, another difficult problem for mobile robots.

Time of flight methods normally depend on ultrasonics or laser beams to illuminate the scene in front of the vehicle. Ultrasonic range finding devices suffer from lack of spacial resolution (30 degrees solid angle beam) and non return of signal off smooth surfaces with normals greater than 40 degrees (from the source beam direction). On top of this, the atmosphere on the planet Mars is too thin to support ultrasonics. Laser range finding devices don't suffer from lack of spacial resolution, non return of signal, or atmosphere limitations. However, laser range finding devices demand precision, high speed electronics to obtain adequate temporal resolution. They also must be capable of handling a large range of light send/receive intervals over a wide dynamic range of reflected light intensity. Laser range finding is difficult to construct properly without even considering data acquisition and processing.

Triangulation-based methods normally depend on laser beams to illuminate the scene in front of the vehicle. Laser triangulation seems best suited to the obstacle detection problem of mobile robots. Laser triangulation suffers from the "missing parts problem" since the detector cannot always "see" what the source beam is illuminating. However, by adjusting the separation between source and receiver, you can achieve a good balance between "missing parts" and range accuracy.

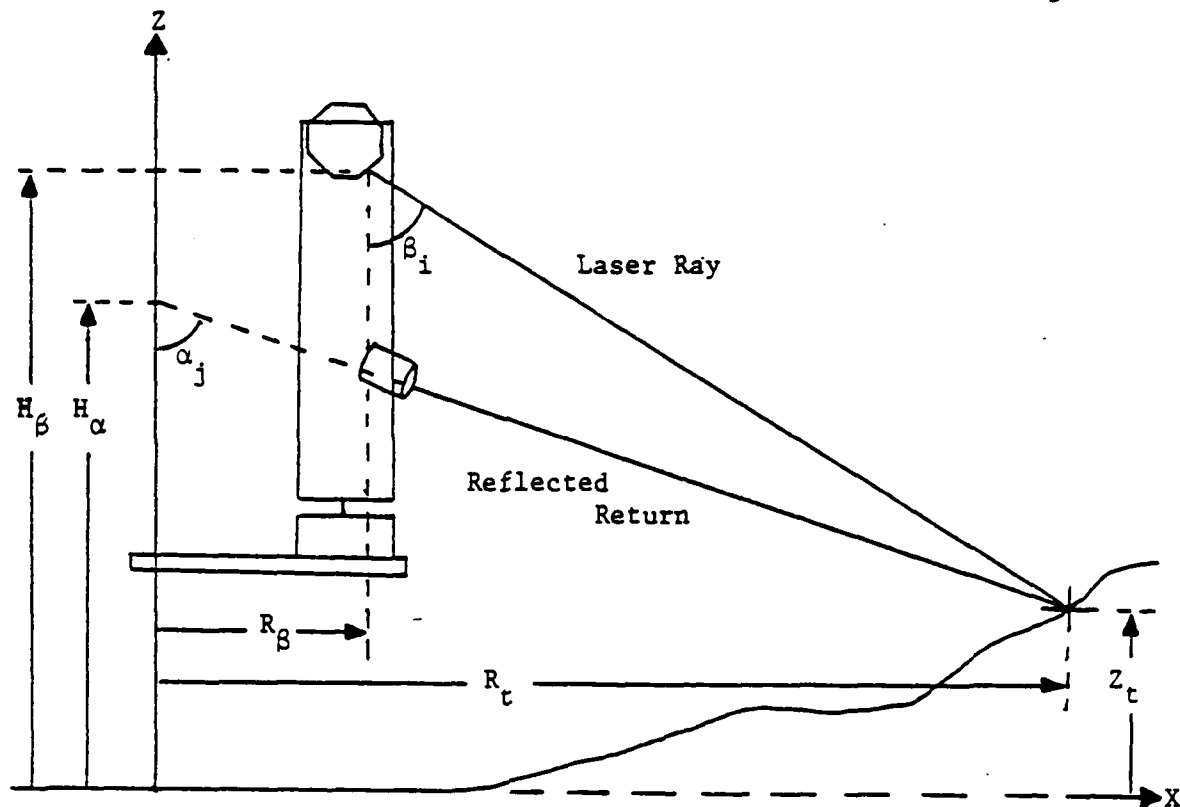
Laser triangulation can provide high resolutions and still be computationally inexpensive. In the area of mobile robots, where real time processing is crucial, laser triangulation excels.

### 1.2 The Multi-Laser, Multi-Detector System

The Mars Rover presently uses a Multi-Laser, Multi-Detector System (ML/MD) for triangulation-based obstacle detection. This ML/MD system was originally designed by J. Craig in 1978 [2], revised by W. Kennedy in 1980 [3], and evaluated by T. McEllis in 1982 [4]. The system uses a 100 watt pulsed 5-element laser diode array as the laser source, and a 20-element linear photodiode array as the receiver.

For each laser shot within the field of view of the detectors, one or two detectors will "see" the reflected return. By knowing the angle of the laser shot, the angle of the detector cone of vision, and the locations of the laser and detectors, the height and range at a terrain point can be calculated using the triangulation equations shown in figure 1 [4].

The ML/MD system scans 32 elevation angles ranging from  $23^{\circ}$  to  $56^{\circ}$  (measured from vertical) for each of 32 azimuth angles ranging from  $-43.5^{\circ}$  to  $43.5^{\circ}$  (measured from dead ahead). The laser strikes level ground at a radius of 0.96 to 3.3 meters from the mast, and the photodiode detector cones intersect level ground at a radius of 1 to 2.8 meters from the mast. Presently, each scan may take a minimum of 560 msec, with a setup time of 1.74 seconds before the beginning of the next scan.



$R_\beta$  = Forward Displacement of Laser Ray Origin

$H_\beta$  = Height of Laser Ray Origin

$\beta_i$  = Elevation Angle of Laser Ray

$\alpha_j$  = Angle of Laser Return "Seen" by Detector

$H_\alpha$  = Effective Z-axis Intercept Height of Reflected Return

$Z_t$  = Terrain Height at Observed Terrain Point

$R_t$  = Terrain Range at Observed Terrain Point

$$Z_t = \frac{H_\beta \tan \beta_i - H_\alpha \tan \alpha_j + R_\beta}{\tan \beta_i - \tan \alpha_j}$$

$$R_t = \frac{\tan \alpha_j [(H_\alpha - H_\beta) \tan \beta_i - R_\beta]}{\tan \beta_i - \tan \alpha_j}$$

Figure 1. Triangulation Equations

This Multi-Laser, Multi-Detector System (ML/MD) is capable of providing terrain information at fast rates, upon which navigational judgements can be based.

### 1.3 Adaptive Suspension Vehicle

During 1982, the Mars Rover Project focused on the evaluation of the Multi-Laser, Multi-Detector System as an obstacle avoidance system for the Adaptive Suspension Vehicle (ASV), and the design of a new generation laser triangulation-based system for the ASV.

The Adaptive Suspension Vehicle (ASV) can basically be described as a six-legged walking vehicle designed to replace the army mule. An enclosed cab space in the front of the vehicle will hold a seated operator, a payload section in the rear will hold gear to be transported, and six legs will control vehicle height and track. The average track of the vehicle is about 1.5 meters, and the average height of the roof is about 2 meters.

Individual short-range detectors for each "foot" will redirect steps when necessary, and the operator will guide the vehicle in a general direction (similar to guiding a horse). The vision system, or obstacle avoidance system will do the following. It will choose an optimal path in rough terrain to stay on course and avoid obstacles, it will alert the operator and/or stop the vehicle if the terrain ahead is impassable, and it will allow the vehicle to follow a trail. This vision system allows the vehicle to anticipate changes in terrain, it frees the operator from controlling individual steps, and it allows operation at night with minimal lighting for the operator.

An infrared scanning system similar to the ML/MD system can provide the ASV with all the information it requires to negotiate rough terrain. However, because of its need to navigate in forested areas and its increased sprint speed (3 meters per second), the ML/MD system needs to be modified.

The author's work, and the subject of this report, is the investigation of new and improved scanning techniques that will increase the scan rate, range, flexibility, and resolution. The bulk of this report is based on extensive research in the areas of electro-optics, acousto-optics, and holographics.

## PART 2

### A NEW MULTI-LASER, MULTI-DETECTOR SYSTEM

The parts of a new ML/MD system that this report is concerned with are the laser, the laser scanner, the detectors, and the scan control electronics. This part of the report discusses a new laser scanner (its scan pattern, and theoretical resolution), and scan control electronics. The laser and detectors are discussed in a later part of this report (Sources and Receivers).

A new ML/MD system has been investigated in an effort to improve the resolution, scan speed, scan pattern, and operation of the current ML/MD system used on the Mars Rover. The author suggests improvements that are best suited to laser triangulation.

#### 2.1 Scanner Description

The laser scanner is responsible for directing laser shots into specific azimuth and elevation angles. The scanner must be fast and accurate. For these and other reasons mentioned in later parts, a holographic scanner was chosen to produce a rapid azimuth scan and a galvanometric scanner was chosen to produce a slower elevation scan.

The holographic scanner should be a 10 facet hologon produced by International Dichromate Corporation. The hologon should be custom built for insensitivity to wobble, high efficiency at 904 nm working wavelength, and focusing at the middle of the ground level elevations (this yields an arc scan). The hologon should be rotated with a synchronous motor in order to coordinate azimuth and elevation scans.

The galvanometric scanner can be purchased complete with control electronics from General Scanning Company. Synchronization to the azimuth scanner can be done simply with a single chip programmable timing module (MC 6840).

Using a Laser Diode Model LD-360 700 W array, the scanner can produce rapid high intensity scans. By firing the laser at 4 KHz (well below its 10 KHz maximum) and 50 ns (.02% duty factor) pulse width, 2000 shots can be produced for each scan at 2 scans per second. With a 40° azimuth scan and 34° elevation scan (40 azimuth shots and 50 elevation shots), the hologon must rotate at approximately 8.67 rps and the galvanometer at approximately 0.19 rps. At these speeds it is obvious that even with continuous scanner rotation the laser pulse "sees" a motionless deflector for all intents and purposes.

## 2.2 Scan Pattern

The laser should be mounted 2 meters above the nominal terrain level, and the detectors should be mounted 1 meter below the laser. The laser should scan 40° in azimuth and 34° in elevation. This yields a scan range of 2 meters to 10 meters, and a scan width of 1.4 meters (at 2 meters) and 7.2 meters (at 10 meters). This large pattern gives the vehicle a good view of the terrain it is approaching. With a laser fire rate of 4 KHz, there can be 2 scans per second with 2000 laser shots per scan. With 40 azimuth shots and 50 elevation shots, there is only 1° between azimuth shots and 0.7° between elevation shots. The detectors have a field of view of 40° in azimuth and 21° in elevation in order to view the scanned area.

At the vehicle's maximum speed of 3 meters per second and the scan speed of 2 scans per second, the vehicle will travel 1.5 meters per scan. This allows 5 full scans to be completed between 2 and 10 meters. That is the vehicle will see a given section of terrain 5 different times at 5 different angles before it must cross that section of terrain. This appears more than adequate for obstacle detection and avoidance.

As with any triangulation scheme, there is a problem with "missing parts". This problem is most difficult when a vehicle must negotiate negative as well as positive obstacles. A positive obstacle can be thought of as a box set on top of level ground, while a negative obstacle can be thought of as a hole or depression below level ground. The negative obstacle proves the most troublesome since this obstacle may not be seen.

With the scan pattern and laser/detector locations described above, the ML/MD system can "see" the bottom of a hole whose depth is one-half its width at 2 meters. With careful obstacle threshold selection this should prove to be no problem since an obstacle threshold of one-half vehicle wheel diameter is presently being used.

### 2.3 Theoretical Resolution

With any triangulation-based system there is a certain amount of uncertainty associated with the calculation of range and elevation of a terrain point. This uncertainty develops because of a finite detector cone of vision, and separation of the laser and

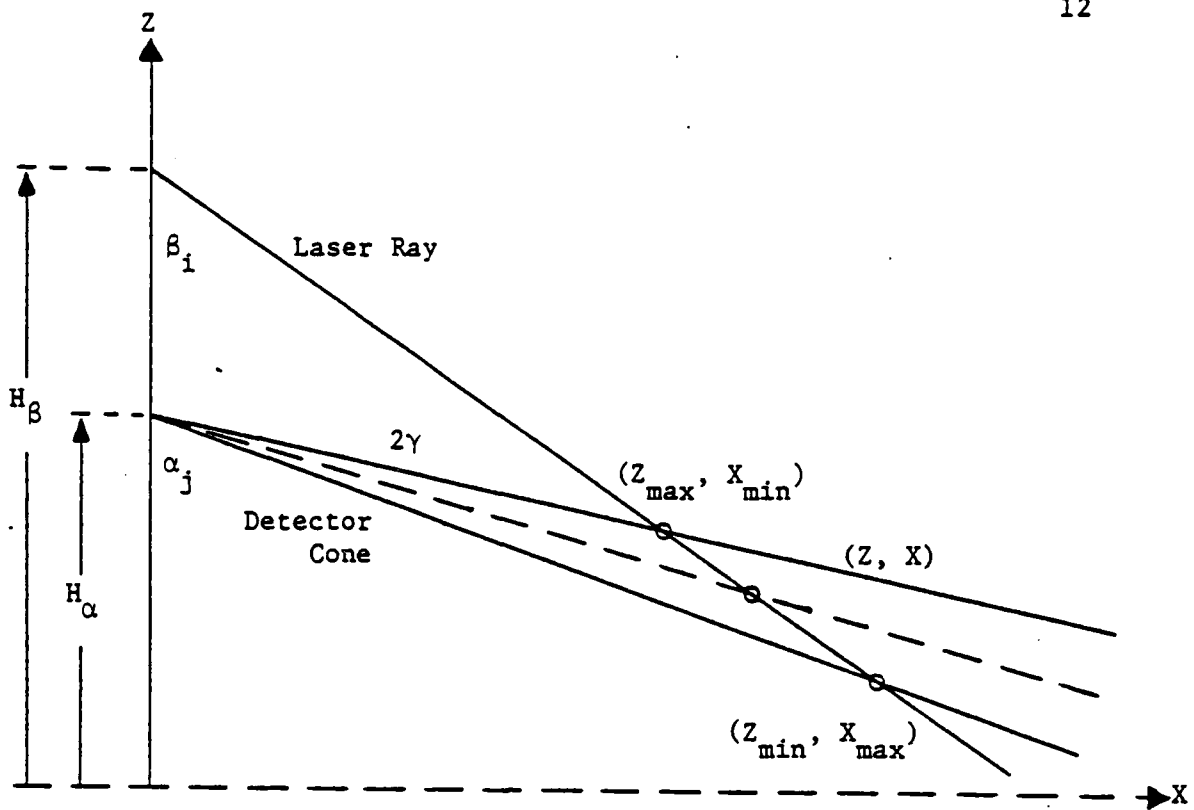
detector. This uncertainty is diagramed in Figure 2, and from the equations can be seen to be directly proportional to the distance between the laser and the detectors. At 2 meters the uncertainty in elevation is 3.6 cm, and the uncertainty in range is 3.6 cm. At 10 meters the uncertainty in elevation is 15.9 cm, and the uncertainty in range is 79.6 cm. This translates to a 1.8% uncertainty in range at 2 meters, and a 7.9% uncertainty in range at 10 meters.

Since the area in front of the ML/MD system is scanned five times, uncertainty decreases with proximity to the ML/MD system, and obstacles are on the order of 25 cm, these uncertainties are of little concern. The uncertainties can be improved by increasing the number of detectors, increasing the distance between the laser and detectors, or by increasing the height of both the laser and detectors.

By changing the distance between the laser and detectors, a balance can be achieved between "missing parts" and uncertainty. The closer the laser and detectors, the greater the uncertainty and the smaller the "missing parts" problem. The farther apart the laser and detectors, the greater the "missing parts" problem and the smaller the uncertainty.

#### 2.4 Control Electronics

The control electronics are used to synchronize the firing of the laser with the azimuth and elevation scanners, and to latch the high and low order detector numbers of excited photodetectors.



$H_\beta$  = Height of Laser Ray Origin

$\beta_i$  = Elevation Angle of Laser Ray

$\alpha_j$  = Elevation Angle of Detector Field of View

$H_\alpha$  = Height of Detector

$2\gamma$  = Detector Field of View

$\Delta z$  = Uncertainty in Height of Terrain Point

$\Delta x$  = Uncertainty in Range of Terrain Point

$$\Delta z = \frac{\tan(\frac{\pi}{2} - \alpha_j + \gamma)}{\tan(\frac{\pi}{2} - \beta_i) - \tan(\frac{\pi}{2} - \alpha_i + \gamma)} - \frac{\tan(\frac{\pi}{2} - \alpha_j - \gamma)}{\tan(\frac{\pi}{2} - \beta_i) - \tan(\frac{\pi}{2} - \alpha_j - \gamma)} (H_\beta - H_\alpha)$$

$$\Delta x = \frac{1}{\tan(\frac{\pi}{2} - \beta_i) - \tan(\frac{\pi}{2} - \alpha_j - \gamma)} - \frac{1}{\tan(\frac{\pi}{2} - \beta_i) - \tan(\frac{\pi}{2} - \alpha_j + \gamma)} (H_\beta - H_\alpha)$$

Figure 2. Triangulation Uncertainty

An MC 6809 microprocessor controls the scanners and collects detector information. A block diagram of the electronics is shown in figure 3.

An MC 6840 programmable timing module sends clock signals to the synchronous azimuth and elevation scanners to control scan speed, and a fire pulse to the laser fire circuitry and detector latches. The programmable timing module has three independent clock inputs and outputs, and (as the name suggests) each can be programmed via three control registers to operate in various modes. In this application the module is programmed for two clock outputs and one pulse output (figure 4). The clock frequencies (and pulse duty factor) are controlled via four registers. Thus the scan speed can be altered readily through software.

In figure 5 the programmable timing module connections are shown. In this configuration the system clock ('E' on the MC 6809) is used as a base for all the counters. Clock 1 drives the elevation scanner, clock 2 drives the azimuth scanner, and clock 3 fires the laser and latches the high and low order detectors after a 300 ns setup delay. A small photodiode mounted just in front of the scanner detects the end of scan and initializes the programmable timing module.

Since 48 different detectors (each with their own amplifier and comparator) are used, priority encoding is done immediately to alleviate the problem of the tremendous amount of data coming from them. Six 74LS148 priority encoders, three 74LS100 nand gates, and two 74LS153 multiplexes are connected as shown in figure 6 to produce the number of the highest order detector seeing a given laser shot.

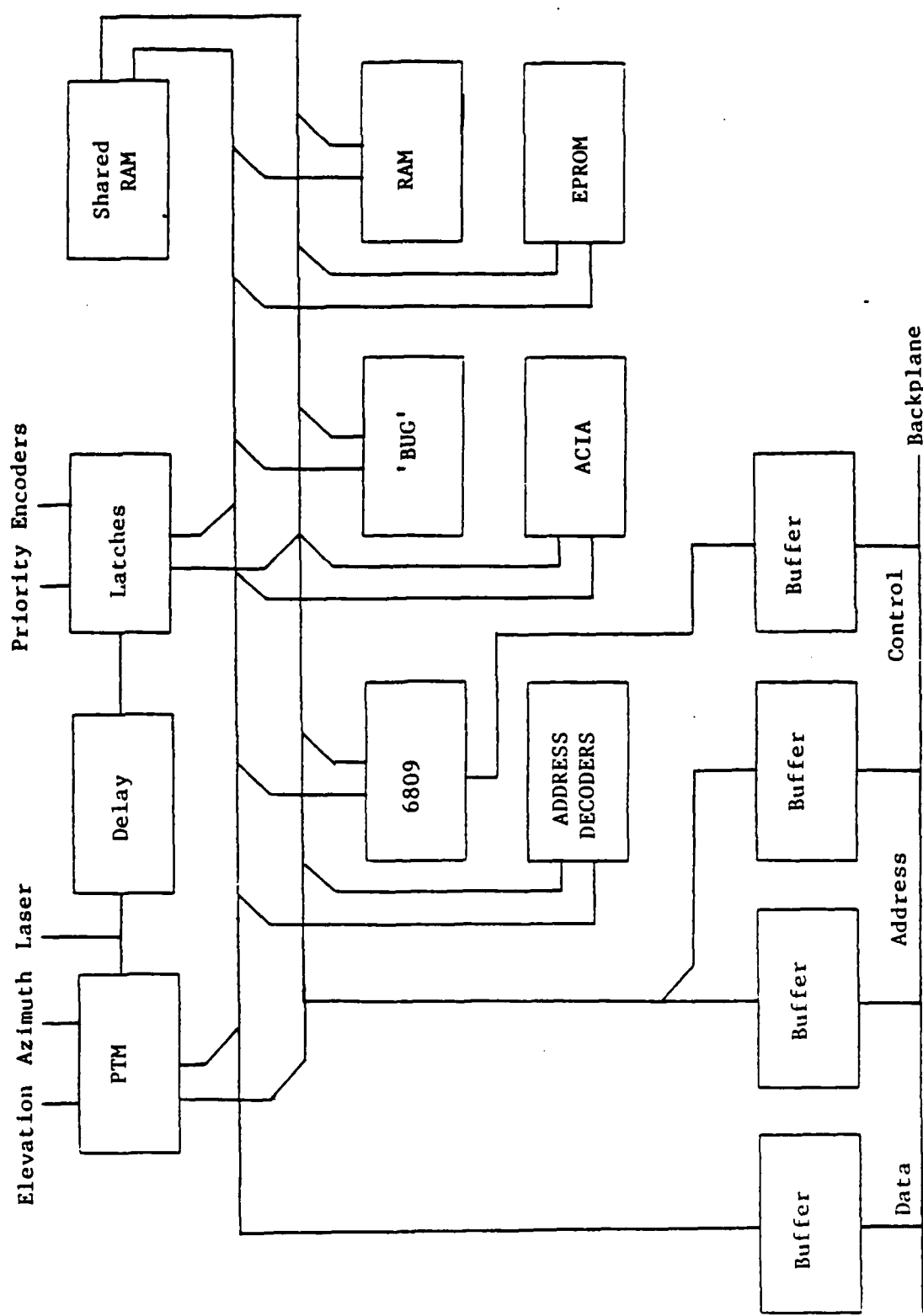


Figure 3. Electronics Block Diagram

$T$  = Period of Clock Input (or E)  
 $N$  = 16 Bit Number in Counter Latch  
 $M$  = Contents of Most Significant Byte  
 $L$  = Contents of Least Significant Byte  
 $TO$  = Counter Time Out

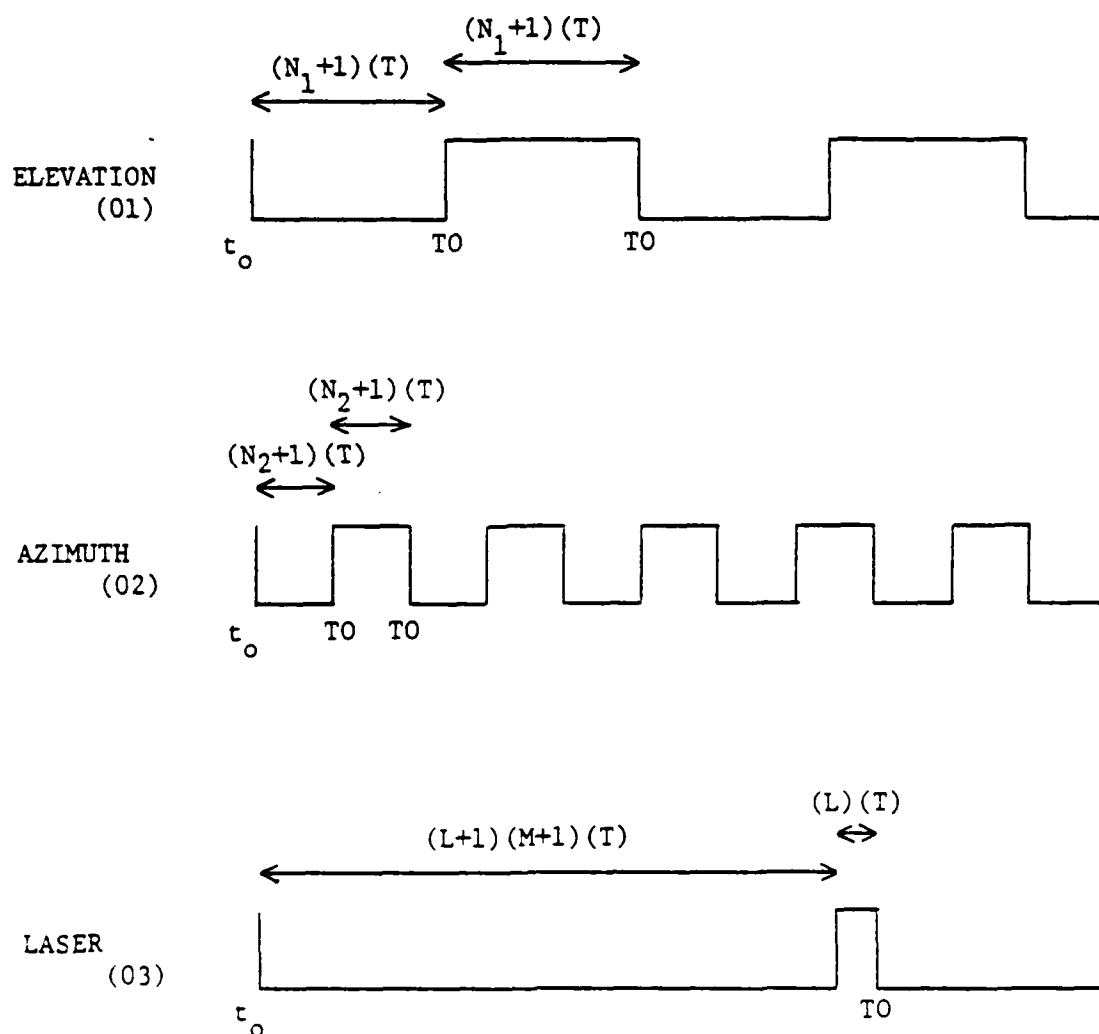


Figure 4. Programmable Timing Module Outputs

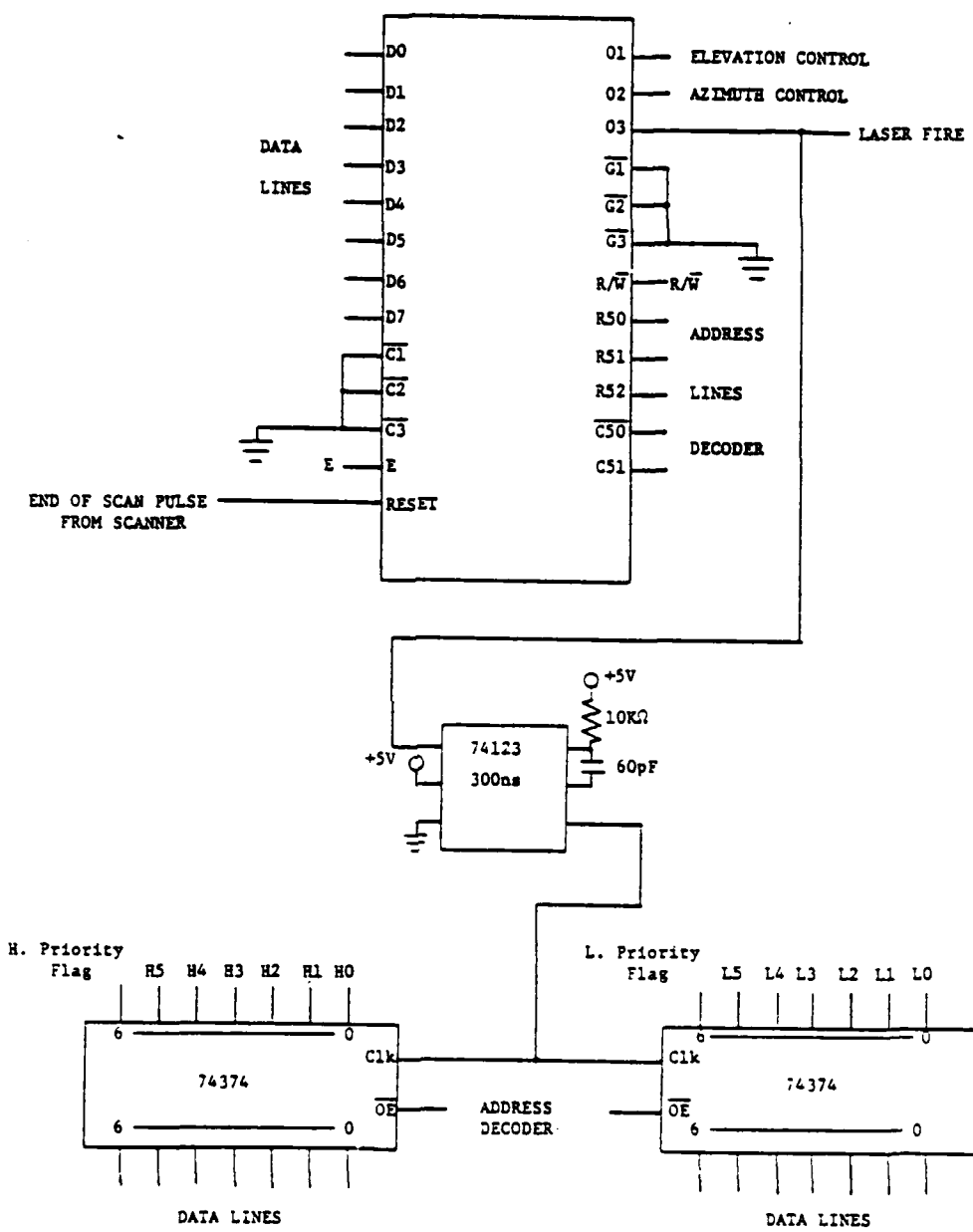


Figure 5. Programmable Timing Module and Detector Latches

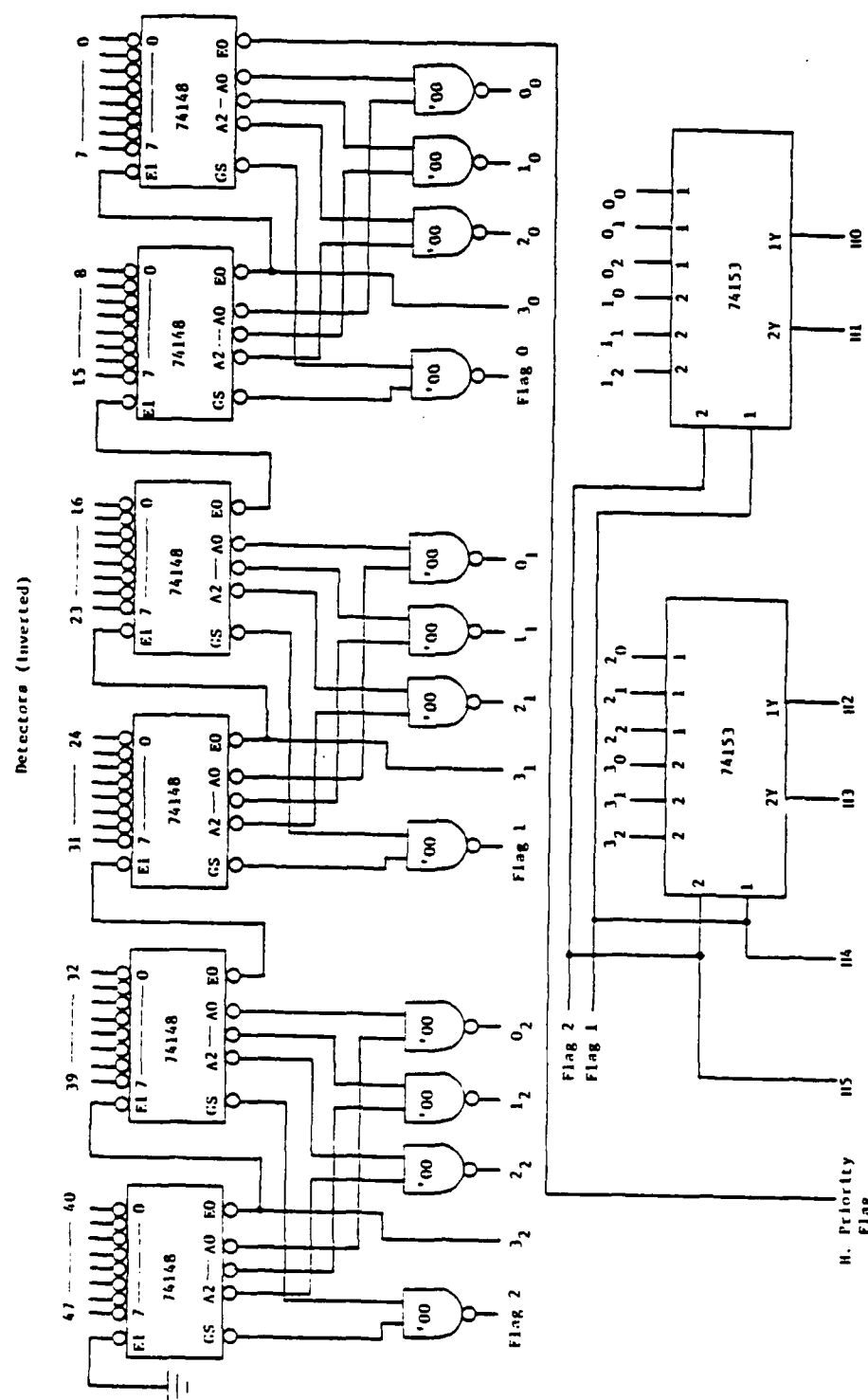


Figure 6. High Order Detection

Similarly, the chips in figure 7 are connected to produce the number of the lowest order detector seeing the same laser shot. The numbers are then latched so that the microprocessor can retrieve the detector numbers when it is ready to do so. When the microprocessor is ready, the detector pair is moved to the shared RAM and then on to the Prime computer for triangulation calculations. This design is easily adaptable to the Mars Rover's present laser scanning system and mast telemetry [3,4].

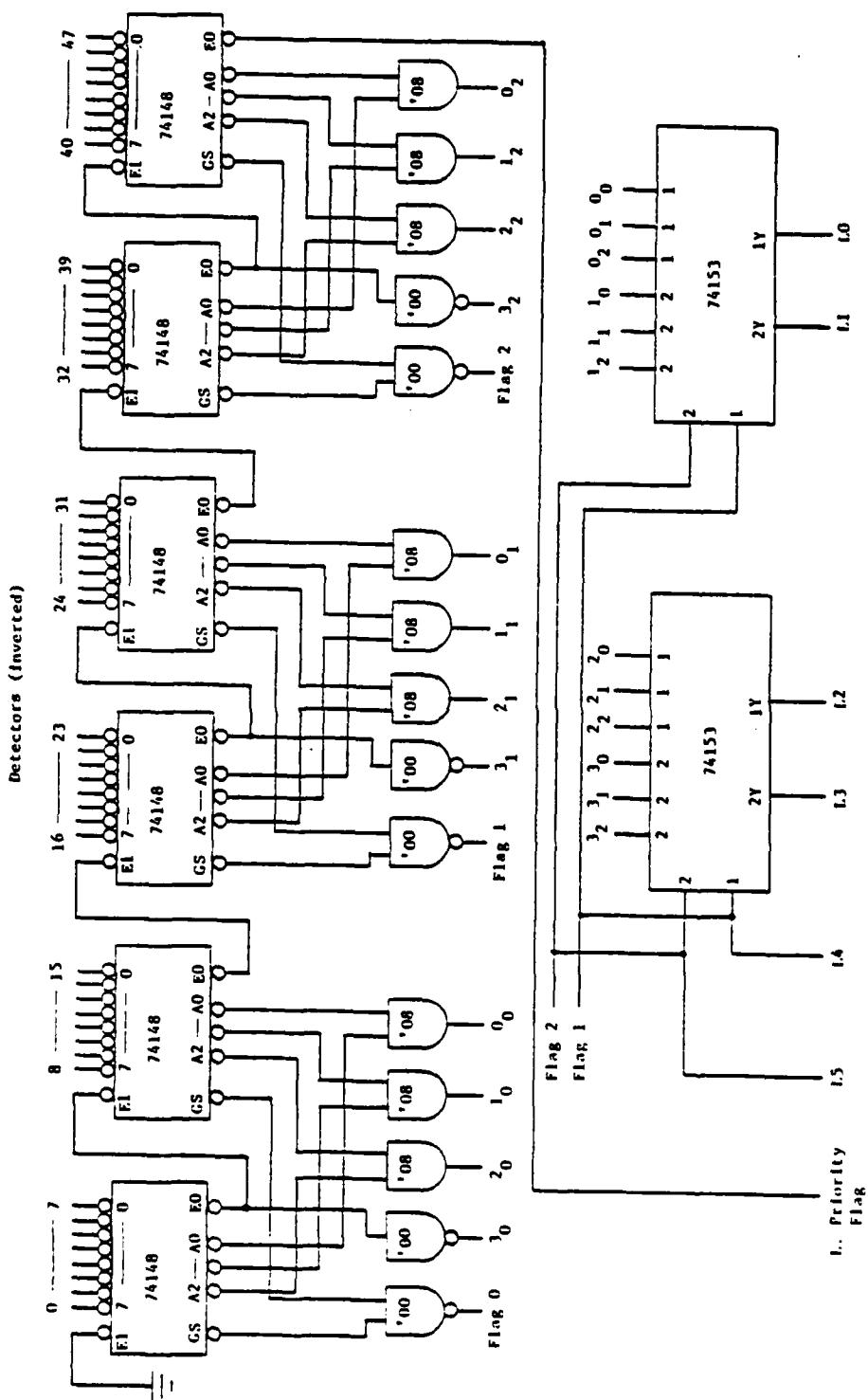


Figure 7: Low Order Detection

## PART 3

### LASER DEFLECTION TECHNIQUES

At the heart of any laser scanner is the deflector necessary to convert the stationary laser beam into some sort of two-dimensional scan. In practice, the use of fast one-dimensional scanning is almost universal. A slow (elevation) scan is generally provided by a detector rotating on an axis orthogonal to that of the fast one-dimensional (x or azimuth) scan. The following discussion will focus on the fast scan, which usually constitutes the critical part of the scanning process.

Some of the basic characteristics of a laser beam deflector are maximum deflection angle, efficiency and angular resolution. By comparing these characteristics and the line-scan rate one can choose the deflection technique best suited to a certain application.

#### 3.1 Mechanical Deflectors

Mechanical deflectors can be divided into two groups suitable for high speed, high resolution scanning: low-inertia galvanometric oscillating mirrors, and high-inertia rotating mirrors. Both still enjoy widespread use in image recording and reproduction.

Galvanometer mirrors are the oldest mechanical deflection technology, and most engineering students have measured small currents with a galvanometer that had a mirror attached to a coil in introductory physics laboratories. The magnetic deflection principle is the same whether the coil is moving or an iron armature is moving (using a fixed field coil).

Galvanometric optical scanners are now available with unloaded natural frequencies as high as 3.2 KHz, and linearities as high as 1% of the working excursion with the use of servo control drivers. The special servo control driver amplifiers allow the galvanometers to follow sawtooth waveforms rather accurately. However, loading the galvanometer with a mirror even as small as 7 x 7 mm reduces the scan speeds tremendously. Typical scan rates approach 150 Hz and typical peak to peak rotations approach 20°, while still maintaining the 1% linearity [5].

Galvanometric optical scanners inherently have high deflection efficiencies (> 90%) and angular resolutions. But these are more than offset by their disappointing scan rates and deflection angles.

The drawbacks of the oscillating type scanners can be overcome by the use of a rotational type scanner. Rotating mirror scanners don't try to overcome the inertia of the scanning mirror. Instead, they make use of the high inertia mirror to produce stable scans.

Rotating mirror deflectors normally use polygonal mirrors to produce fast scan rates. The rotational rate of polygon scanners is limited only by material deformation or failure considerations and polygon size. The deflection angles of the polygon scanner are only limited by polygon size.

Thus rotating mirror deflectors can provide large deflection angles, high deflection efficiencies, high angular resolutions, and

high scan rates. However, there are drawbacks to polygon scanners. The drive/control system for a polygon scanner can become bulky and awkward to implement for high speeds and large deflection angles. And in order to reduce scan wobble produced by polygon wobble, precision bearings and/or special optics must be used.

### 3.2 Electro-Optics

Because of the drawbacks of mechanical scanners, much work has been done in the area of solid state deflectors. Any scanning technique that depends on the physical motion of a reflecting surface is restrained to sequential scanning. However, this does not hold true for solid state deflectors. These deflectors have no moving parts, have speeds characteristic of electronic devices, and are not restrained to sequential scanning. One of these solid state deflectors falls under the realm of electro-optics.

A light beam propagating through a prism is deflected by an amount proportional to the prism's shape, orientation, and refractive index. By altering any one of the above characteristics of a prism, you can alter the deflection of a light beam. To alter the orientation of a prism you need some mechanical device, and to alter the shape of a prism is a difficult task to say the least. However, it is rather simple to alter the refractive index of an electro-optic material such as barium strontium niobate.

A digital light beam deflector has been developed that consists of several binary deflection units (figure 8) [6]. Each deflection unit can deflect a light beam into two different directions.

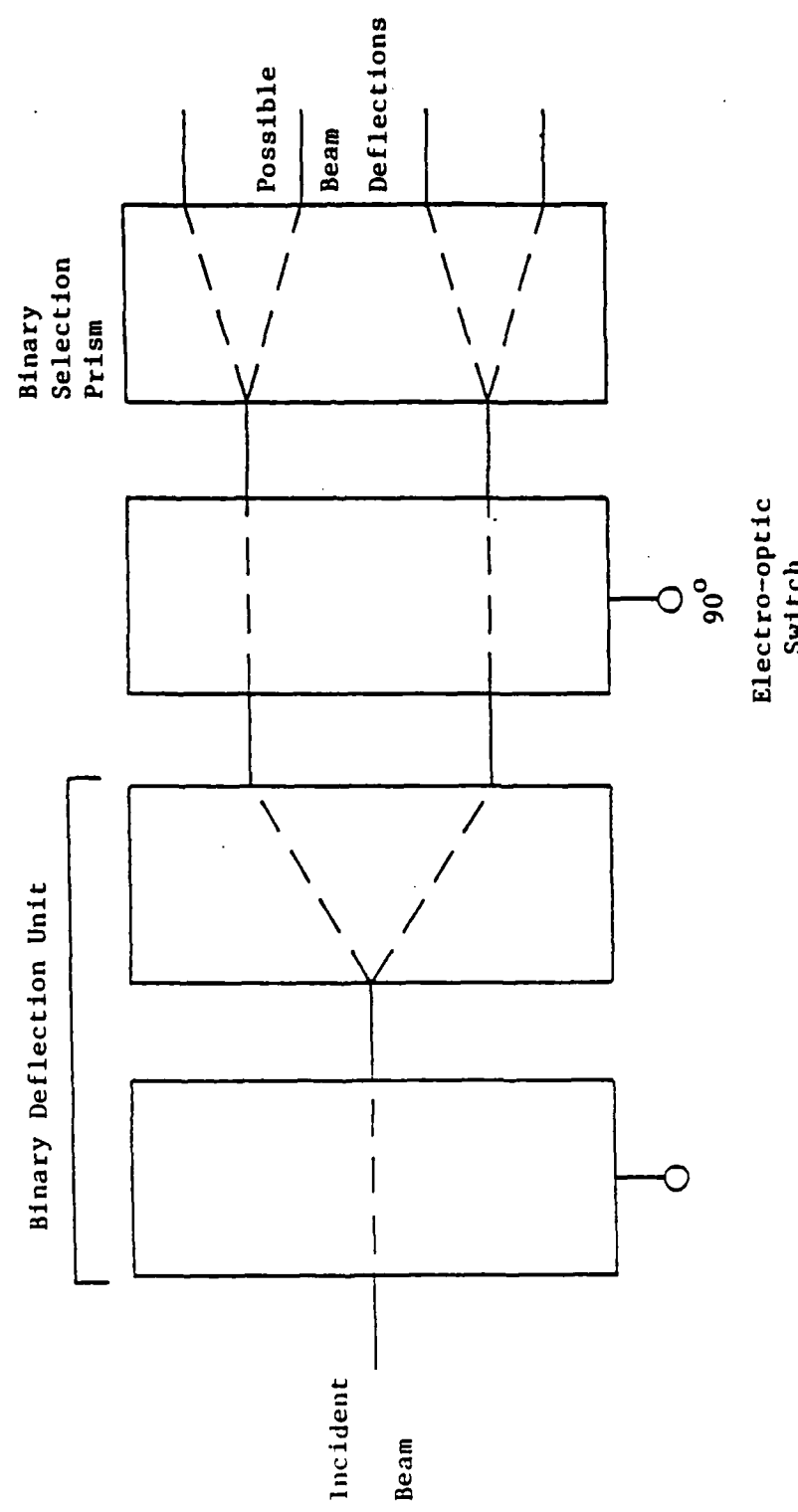


Figure 8. Electro-optic Deflector

You can produce  $2^N$  different deflections by positioning N diffraction units in cascade. The binary deflection unit consists of an electro-optic crystal and a birefringent prism. Light entering the prism will be deflected in one of two directions depending on its polarization. By applying certain voltages to electro-optic crystals you can change the polarization of a light beam passing through the crystal.

There are two major drawbacks to the use of electro-optic crystals for light beam deflection. The large number of surfaces in a deflection system cause extremely low light throughput efficiencies, and deflection angles are inherently small. To increase the range of deflection angles you must increase the number of deflection units, decreasing the throughput efficiency.

### 3.3 Diffraction

Up to now the discussion has been the deflection of light by means of reflection and refraction. Light can also be deflected by means of diffraction. Light can be diffracted by means of physical or acoustical diffraction gratings, into a set of multiple beams or orders. The angle of deflection of the beam is given by

$$\sin\theta = \frac{m\lambda}{d}$$

where

$m$  = the order of interest

$\lambda$  = the light wavelength within the diffraction medium

$d$  = the grating spacing and/or the acoustic wavelength within the medium.

### 3.3.1 Acousto-optics

Acousto-optical deflectors diffract light beams by forming a phase grating in an optically transparent material with an acoustic wave. The phase grating is formed by a refractive index change due to the photoelastic effect; the strength of the change depends upon the sound amplitude and the magnitude of the photoelastic effect of the particular medium.

RF signals ranging from 40-300 MHz are applied to a piezoelectric transducer bonded to the acousto-optical material, setting up a standing sound wave in that material. Amplitude modulation of these RF signals gives rise to intensity changes in the diffracted and undiffracted beams.

Depending on the thickness of the acousto-optic material (and thus the thickness of the sound field) the acousto-optical deflector operates in either the Bragg or Raman-Nath regime of acousto-optic interaction. The intensity of each diffraction order depends on the thickness of the sound field, thus it is important to consider each regime. In the Raman-Nath regime (thin sound field) the acoustic grating phase modulates the input wave front creating orders that follow the Bessel series (similar to phase modulation of an RF carrier). In the Bragg regime (very thick sound fields) only the zeroth and first order diffraction orders exist. Since only two diffraction orders exist, the intensity of the first order diffraction angle is much greater than it would be for the Raman-Nath regime (many diffraction orders) [7].

Here we see that Bragg diffraction is the more useful for laser scanning. By blocking the zeroth order diffraction beam, scanning can be accomplished with the first order beam by altering the acoustic frequency.

The driving circuitry for an acousto-optical deflector is very similar to that of an FM radio transmitter. The typical power required is 1-2 W, and since typical piezoelectric transducers have a  $50 \Omega$  impedance, peak to peak driver voltages range 20-30 V. The acousto-optical cell is relatively insensitive to temperature, and does not require the use of polarized light. The acousto-optical scanner provides extremely high resolution and scan rates. However, the acousto-optical scanner is not without drawbacks.

The access time (or the time needed to fill the cell with a given frequency) depends on the diameter of the incident light beam because of the propagation of the traveling wave across it. Thus to achieve the high speed scanning it is important to focus the light beam in the cell. However, in practice, a focussed beam causes a reduction in diffraction efficiency, and this makes it more difficult to distinguish zeroth and first order diffraction angles. To alleviate the problem of distinguishing orders, higher acoustic frequencies are required. But the reduced diffraction efficiency still exists. Another problem is the small deflection range. Acousto-optical deflectors can only offer a maximum deflection angle range of three degrees. This, along with a very small diffraction

efficiency into the first order (< 40%), has kept acousto-optical deflectors behind mechanical deflectors.

### 3.3.2 Holographics

Up to now only one new technology has arisen that can compete with the resolution and speed available from polygon scanners, and that is the rotating hologon. The hologon is a holographic, diffractive, optical element scanner. The rotating hologon uses the same principle as the high-inertia rotating polygon mirror, except that the hologram replaces the polygon facets with diffractive elements or holofacets. This seemingly trivial difference leads to some important scanning differences.

First of all a hologram of a fixed period diffraction grating can generate a scan line by rotating it past a stationary light beam. This produces a scan action similar to rotating a wedge-shaped prism, or to rotating a tilted mirror around an axis forming an acute angle to the mirror normal. In this simple case, the scan motion is inherently circular.

Thus a hologram mounted on a disc can be rotated past a light beam to produce a scan. This holographic disk has less wind friction, suffers negligible distortion from centrifugal forces (even at high rotational speed), and is inherently better suited to create two- and even three-dimensional scans.

Other advantages of holographic scanners are more directly related to their formation. Holograms are easy to manufacture and replicate, implying low cost. Transmission holograms can also be

made almost insensitive to motor bearing and mounting wobble or surface tilt by selecting optimal geometries.

In a few years holographic scanners should replace polygon scanners in many applications. In the area of laser triangulation for obstacle detection, holographics offer the best method for laser scanning to date.

## PART 4

### HOLOGRAPHIC DIFFRACTION GRATINGS

There are hundreds of holograms on the market today ranging from colorful reflection hologram pendants to complex transmission hologram configurations. The bulk of the author's research has been in the area of holographic diffraction gratings and their application to laser beam deflection.

The following discussion focuses on high efficiency hologram types, hologram formation in a certain high efficiency material, and a currently available high efficiency holographic scanner.

#### 4.1 Classification of Holograms

There are two characteristics important to the formation of high efficiency holograms: the type of medium used (medium thickness), and the particular wave parameter being recorded (amplitude and/or phase). These two characteristics determine the efficiency of a given hologram.

##### 4.1.1 Thick Films Versus Thin Films

If, in the recording of interference fringes, the recording uses only the surface of the medium, or if the thickness of the recording medium is small compared to the fringe spacing, a thin (or plane) hologram is recorded. If the three-dimensional interference pattern is recorded and used in depth, or if the recording material is on the order of or greater than the fringe spacing, a thick (or volume) hologram is recorded. The distinction between the two is usually made

with the aid of the Q-parameter defined as [8]

$$Q \equiv \frac{2\pi\lambda T}{n d^2}$$

where

$\lambda$  = illuminating wavelength

T = thickness of the recording material

n = index of the recording material

d = spacing of the recording fringes.

For  $Q < 0.1$  the hologram is thin and diffraction is in the Raman-Nath regime as discussed in part 3. For  $Q > 10$  the hologram is thick and diffraction is defined by thick hologram theory (coupled wave theory) or is said to be in the Bragg regime as discussed in part 3. As discussed before, it is obvious that the thick film hologram is the choice for laser scanning.

In volume, high diffraction efficiency holograms, the incident wave is strongly depleted as it passes through the grating. The coupled wave theory takes into account that at some point within the grating there are two mutually coherent waves of comparable magnitude traveling together. The coupled wave theory assumes that there are only two waves present: the incident wave, and the diffracted signal wave. It is also assumed that the Bragg condition is approximately satisfied by these waves and that all other orders strongly violate the Bragg condition and thus are not present. For a complete treatment of the coupled wave theory refer to [9]. The grating provides the diffraction coupling between the incident wave and the

diffracted wave, and energy interchange occurs as the waves move through the grating.

#### 4.1.2 Phase and Amplitude Modulation

A hologram can either modify the amplitude or phase of an incident wave or both. This is similar to amplitude modulation (AM) or phase modulation (PM) of temporal signals [10].

An amplitude hologram amplitude modulates the incident wave, and has an interference pattern recorded as a density variation of the recording medium. The diffracted signal wave, after propagating some distance, gives rise to waves going in three directions. One of these waves is proportional to the incident wave. For an amplitude hologram, the transmitted amplitude depends on the initial exposure, since exposure causes a variation of the absorption constant of the material.

A phase hologram phase modulates the incident wave. The phase modulation can be accomplished by causing the index of refraction or thickness of the hologram to vary with  $x$ . The phase will vary with  $x$  since the optical path is a function of  $x$ , and the phase is a function of the optical path. In certain materials the thickness and/or index of refraction will change as a function of exposure.

It can be shown with coupled wave theory that phase holograms can obtain higher diffraction efficiencies than amplitude holograms [9].

## 4.2 Dichromated Gelatin Films

Dichromated gelatin is the most widely used material in forming high efficiency, volume phase holograms. More importantly, dichromated gelatin possesses almost ideal properties for phase holograms. A large index change can be produced in the interior of the gelatin, making possible volume phase holograms with efficiencies close to 100%.

### 4.2.1 Mechanism of Hologram Formation

Dichromated gelatin and other dichromated colloids are among the oldest photographic materials. Since 1830 it's been known that ultraviolet or blue light can cause cross linking of gelatin molecules in the presence of dichromate. In photographic and printing applications, industry emphasized the thickness variation of the gelatin during processing for image recording. Areas exposed to light form a "resist", meaning they resist a subsequent processing step. The nonexposed areas are washed away or transmit an etchant.

To be used as a resist, a gelatin layer is formed on top of a substrate. Then the exposed areas become cross linked, or hardened, and are relatively insoluble. Development is done in warm water where unexposed areas are washed away. The gelatin and substrate is now placed in an etchant bath, the transmission rate at the etchant through the gelatin varies with thickness, and thus the etch rate of the substrate also varies. In this way continuous tone images are made in the substrate. In a similar fashion, relief type holograms

can be produced. In relief holograms the variation of thickness produces the main optical phase shift. However, the diffraction efficiencies and diffraction angles in relief holograms are small compared to the efficiencies producible in thick, Bragg holograms. In Bragg holograms the phase shift takes place in the interior of a dichromated gelatin plate.

To produce very high-quality Bragg holograms the gelatin film is first hardened so that gelatin is not washed away during sensitizing or development. The degree of hardening is important for if the gelatin is hardened too much, it will no longer deform and become insensitive.

The hardened gelatin is sensitized by soaking in 5% ammonium dichromate. The hardened gelatin swells and absorbs about five times its own volume of water. The gelatin is then air dried. The water evaporates and the dichromate concentration in the gelatin reaches 25 to 30%. The gelatin is now sensitized and ready for exposure.

For hologram formation the film is not exposed uniformly, but rather sinusoidally from the interference of two incident waves. During exposure, absorbed light reduces the  $\text{Cr}^{+6}$  ion to  $\text{Cr}^{+3}$ . Thus the  $\text{Cr}^{+3}$  ion is concentrated periodically within the gelatin. The hologram can now be developed.

During development, areas are hardened relative to the amount they are exposed. This sets up a periodic strain within the gelatin. In the final step of development, the film is rapidly dehydrated in 100% isopropyl alcohol. The strain increases until it

is relieved by the formation of tiny cracks or voids around the unhardened gelatin. Since gelatin molecules (collagen) resemble tiny strings, the voids can be seen as tiny vacuoles. In the area containing gelatin and vacuoles the index of refraction is reduced. Thus the volume phase grating is formed. And since the vacuoles are tiny compared to the wavelength of light, the index of refraction varies rather smoothly in the transition regions [11,12,13].

#### 4.2.2 Diffraction Efficiency

A properly recorded and processed dichromated gelatin hologram has so little light absorption and scattering that it appears almost clear under ordinary room light. These holograms have diffraction efficiencies approaching their theoretical limit of 100%. However, the hologram alone is rather flimsy and easily erased in humid environments. Therefore the hologram is most commonly sandwiched between two glass plates for protection and support.

It has been shown theoretically and experimentally [11] that the diffraction efficiency of dichromated gelatin depends upon the recording wavelength and the exposure. For example, at 488 nm incident wavelength, highest efficiency is achieved with an exposure of  $60 \text{ mJ/cm}^2$ , and at 514.5 nm incident wavelength, highest efficiency is achieved with an exposure of  $250 \text{ mJ/cm}^2$ . Proper recording and processing is essential for maximum efficiency.

Since the holograms are mounted in between glass disks for scanner applications, the efficiency is less than the theoretical 100% value. And because of dichromated gelatin's extreme sensitivity

to variations in processing, maximum efficiencies are difficult to obtain.

A company called International Dichromate Corporation (IDC) has begun to produce holographic scanners with some outstanding results.

#### 4.3 IDC's Holographic Scanners

International Dichromate Corporation is currently producing holographic scanners with diffraction efficiencies as high as 80% without anti-reflection coatings. IDC's holographic scanners are sandwiched between two glass disks and sealed with epoxy for protection. The scanners can stand temperatures ranging from less than 0 to 100°C, and specially manufactured scanners can withstand speeds over 6,000 rpm's. The scanner can also be cleaned with ordinary glass cleaners or solvents.

IDC produces a 10 facet holographic scanner with useable scan angles of 46° (only 2° are wasted between facets). IDC will also make special scanners upon request. Such as: scanners for specific wavelengths of light, scanners insensitive to wobble, large scanners with up to 36 facets, scanners that produce a line, scanners that focus and scan light beams in an arc, and scanners with varying efficiency. As long as the scanner requirements are physically realizable, IDC can manufacture it.

## PART 5

### SOURCES AND RECEIVERS

Besides the scanner, two other components are crucial for the effective operation of a laser triangulation system: the laser source, and the photodiode receiver. The laser source must have enough power to produce a "visible" scan pattern. A "visible" scan pattern is one bright enough to be distinguished from ambient light by the viewer (in this case the viewer, or receiver, is a linear photodiode array). And the receiver must have high enough resolution to be able to detect terrain hazards for the vehicle, and should have high enough sensitivity and dynamic range to relieve some of the burden on the laser source.

Laser sources, and photodiode detectors are rapidly changing and improving. In the following sections, the discussion focuses on a few state of the art laser diodes and photodiode detectors.

#### 5.1 Laser Diodes

Since its invention in 1962, the solid state injection laser diode has usually taken a back seat to the gas laser. But here in laser triangulation, the laser diode excels. Since the laser diode can be fired by applying a current pulse, there is no need to modulate the laser beam to obtain discrete points in a scan (this would have to be done if a continuous wave laser were used). Since the duty factor of a laser diode is small (less than 0.1%), high peak power output pulses (up to 1200 watts) can be obtained with much less power than

that required of continuous wave lasers. Finally, high power laser diodes are small and do not require cooling systems to operate; another large advantage over continuous wave lasers.

Laser light differs from that produced by any other source. Ordinary light is a mixture of a wide range of wavelengths emitted in all directions. Laser light is coherent, that is the emitted waves are in phase. Three other characteristics distinguish lasers from ordinary incoherent light sources: narrow emission wavelength (monochromaticity), high directionality, and high intensity.

Although the solid state injection laser diode differs greatly from the gas laser, it is in fact a true laser since it has the four characteristics described above. Lasing action has been achieved with a wide variety of semiconductor materials, but the only practical room-temperature devices being manufactured today are based on gallium arsenide. These laser diodes can convert current directly into light with efficiencies approaching 100%.

Gallium arsenide emits light at a nominal wavelength of 904 nm, has extremely high power densities (up to 5,000,000 watts per square centimeter of emitting facet), and is extremely fast. The rise time of the radiant flux of a pulsed laser diode is typically less than 0.5 ns. Gallium arsenide is inherently much faster than silicon and is now being developed as a next stage in integrated circuit technology.

The nation's leading manufacturer of gallium arsenide injection laser diodes is Laser Diode Laboratories in New Brunswick,

New Jersey. Their typical high power laser diodes have the following characteristics: emission wavelength of 904 nm, spectral width of 3.5 nm, maximum pulse width of 200 ns, duty factor of .02% to 0.1% (with thermal electric cooling), coherence of 2-3 mm, beam spread at half power of 20° parallel to diode junction (28° perpendicular to junction), and a total peak radiant flux of 300-1200 watts. The present scanning system is using an LD-215 laser diode with peak radiant flux of only 100 watts. A special laser diode pulser for these high power laser diodes is manufactured by Power Technology Incorporated in Little Rock, Arkansas ("ILA Series Laser Diode Array Pulser").

### 5.2 Photodiode Detectors

In laser triangulation, a vertically arranged linear array, or linear grouping of detectors has proved to be the most efficient. A single detector gives little range and elevation information, and an area array (or arrangement) is slow, bulky, and yields no more information than a linear array (or arrangement). With clever optics a linear array can act the same as an area arrangement and remain stationary. Detectors can be divided into two groups: photodiode detectors, and CCD photodiode detectors.

The CCD (Charge-Coupled Device) photodiode (also known as CCPD) detectors are merely an extension of CCD shift registers. A charge-coupled device is a semiconductor device in which finite isolation charge packets are transported from one location in a

semiconductor to an adjacent location by sequentially clocking an array of gates. The charge packets are minority carriers with respect to the semiconductor substrate [14,15].

CCD photodiode detectors are available with 64 to 2048 diode elements, and these elements usually measure  $17 \times 17 \mu\text{m}$ . Light incident on the diodes is converted to electric charge which is integrated on the diode capacitance. With a transfer pulse, the charge on all the diodes is emptied into the corresponding elements of a CCD analog shift register. Information can then be shifted out of the register in a serial fashion at rates as high as 20 MHz.

The CCD photodiode detector obviously offers extremely high resolution; however, where high sensitivity and dynamic range are also required, the CCD photodiode detector is poorly suited. The maximum sensitivity available is only 3.5 V per  $\mu\text{J}/\text{cm}^2$ . Considering the size of each photodiode, this sensitivity is not drastically smaller than that available with individual photodiodes. However, to take advantage of this, each triangulation point (or spot of light) must be focused entirely on one element and one element alone. This is not a trivial problem, and in the event that there are fewer laser points than detector elements, much of the detector is wasted. Thus the low sensitivity of the CCD photodiode detector is indeed a problem.

The maximum dynamic range available with CCD photodiode detectors is a disappointing 2500:1. This is most important when there is a large amount of background noise, or poor reflection of the laser points. Unfortunately, high background noise and poor

reflection is the rule rather than the exception for mobile robots.

There are other problems with CCD photodiode detectors. Their integrating nature increases the amount of background noise accumulated with each laser shot. And for each laser shot the entire CCD shift register must be emptied. This makes the integration time a minimum of 13  $\mu$ s, using a 256 element array and 20 MHz data rate. This is considerably longer than the maximum laser pulse width of 200 ns.

Fortunately, standard photodiode detectors are much better suited to laser triangulation. Photodiode detectors are available individually, individually with built in amplifiers (phototransistors), in 2 element linear arrays, in 20 element linear arrays, at the end of optical fibers, and various other arrangements. Most photodiodes have a nominal sensitivity of 0.43 A/W. This can easily be amplified by a single operational amplifier in a current to voltage configuration. With an 82 K $\Omega$  feedback resistor, the sensitivity translates to 35 KV/W or 32 KV per  $\mu$ joule/cm<sup>2</sup>. High efficiency phototransistors have sensitivities of 5 MV/W or 4.6 MV per  $\mu$ J/cm<sup>2</sup> (for 900 nm incident light). This is substantially greater than that of CCD photodiode arrays. The dynamic range of photodiodes is typically 1,000,000:1, also substantially greater than that of CCD photodiodes. Also, photodiodes are usually not used in the integrating configuration of the CCD photodiode arrays. Typical response times of photodiodes are on the order of nanoseconds.

Unfortunately, photodiode arrays do not come any larger than 20 elements per chip. Thus detectors must be combined in some fashion to increase receiver resolution. Photodiodes or phototransistors coupled to fiber optic cables is one solution to this problem. By using fiber optic cables, several detectors can be arranged in an apparent linear array. The detectors can be mounted in a remote location while one end of the fiber optic cables are positioned to form a linear array. Fiber optic cables are practically lossless over short distances, and the only losses might occur in the connection of the fiber to the detector. Commercially produced detectors with attached fiber optics have minimal losses in the fiber-detector connection. Thus single detectors and fiber optic cables provide an excellent means of laser spot detection for triangulation.

### 5.3 Optics

In most receivers lenses are used to focus light onto the detectors. With a vertical linear array, a receiver would have to move with each azimuth in order to keep a maximum amount of laser light impinging on the detectors. However, light can be gathered from a wide angle and concentrated on a linear array. This can be done by using a demagnification rather than a focusing scheme. Demagnification can be observed by looking through a telescope backwards.

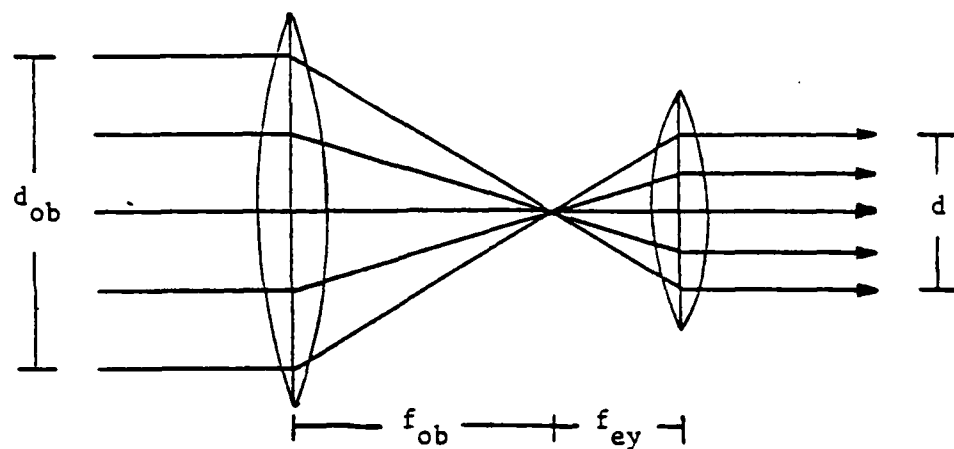
Using demagnification,  $45^{\circ}$  of azimuth can easily be concentrated on a linear detector array. This must be done with cylindrical lenses since the array is not square. Other cylindrical

lenses can be used to focus elevation angles onto different detectors as is more commonly done in both dimensions [4]. Demagnification equations can be seen in figure 9.

When choosing lenses for a receiver, it is important not to use compound lenses containing Canada balsam since this greatly attenuates light at wavelengths around 904 nm. Crown and flint lenses are the best suited for operation at 904 nm.

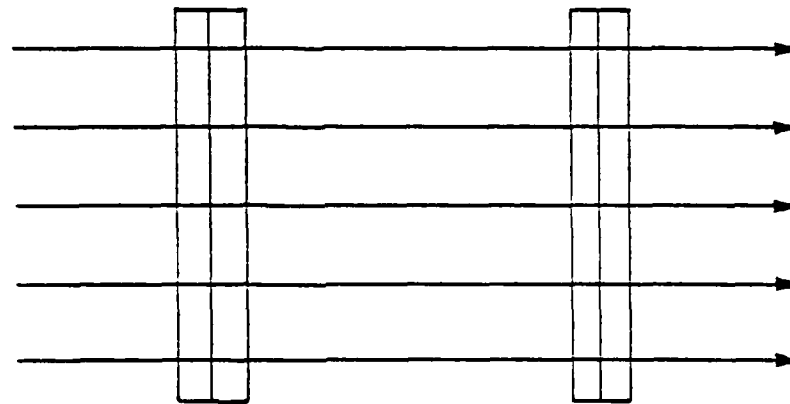
There are several consulting firms that can design the optics for the receiver. Two such firms that might do the design are Block Engineering and Coherent Radiation/Tropel Division.

## Azimuth - Demagnification



$$d = d_{ob} \frac{f_{ey}}{f_{ob}}$$

## Elevation



no effect

Figure 9. Lenses and Equations

## PART 6

### CONCLUSIONS

This report has discussed new scanning techniques and shown the feasibility of these in a new ML/MD laser triangulation system. A holographic scanner is used for rapid azimuth scanning, a galvanometric scanner is used for elevation scanning, special optics and optical fibers are used with individual detectors, a high power laser diode is used as the laser source, and a microprocessor and programmable timing module are used to control the system operation. Each element in the system is an improvement over existing scanning elements. And when a prototype is constructed, the author is fairly confident that the improvement over the existing ML/MD system will be tremendous. The new system should demonstrate higher scan rates, higher efficiencies, greater scan ranges, faster data collection, and greater flexibility.

The holographic scanner should prove to be significantly better than the present rotating mast for laser scanning. Holographic scanners have already been used in supermarkets for quite some time and their speed, accuracy, and ease of operation are unparalleled. From bench tests (using a red laser and an appropriate holographic scanner), the holographic scanner appears to exhibit higher scan stability, and easier operation than the current system. This along with several papers documenting the high efficiency and flexibility of holographics, indicates that holographic scanning is the technique of the future.

The receiver incorporates several improvements. A new optical system allows the receiver to remain stationary. The improvement here is obvious, why rotate the receiver if it is not necessary? Fiber optics allow new high efficiency photo transistors to be used in remote locations, rather than the lower sensitivity photodiode arrays. With the addition of an optical high-pass filter, background noise can be substantially reduced. Because of the low-pass characteristic of silicon photodiodes, a high pass filter creates a band-pass effect. High efficiency optical filters can be purchased from optical firms such as Orion or Melles-Griot.

The laser source very simply provides a seven-fold increase in the available light power. This increase in light power should increase the intensity of the reflected light seen by the detectors. The light emitted from the laser is highly directional, and its intensity can be assumed to be constant over distance in this application. Although the laser beam enlarges with distance, the detector's cone of vision also enlarges with distance. As long as the laser beam size is smaller than the detector cone size at a given distance, no light will be lost outside of the detector cone. Because of the laser spread being smaller than the detector spread, the laser intensity can be assumed constant with distance.

As the laser light strikes an object, light is reflected in all directions. This dispersion of light can be modeled as a point source, at large distances from the detectors. Now the intensity of light emitted from a point source is not at all constant with

distance. As the light travels in all directions, the intensity (or power per solid angle) decreases. This change in intensity of the reflected light follows an inverse square law. That is, the intensity of the reflected light is inversely proportional to the square of the distance from the reflection point.

With the above arguments, scan range can now be investigated. The new system proposes a 700 watt laser diode and an increase in scan range to 10 meters. Currently, a 100 watt laser diode is used with a scan range of three meters, and weak reflections are not a problem. The intensity of the light reflected back to the detectors at 10 meters (using the 700 watt laser diode) can be found to be on the same order as the intensity of the 100 watt reflection at three meters. With the improved detectors, even stronger signals can be expected from the greater range.

The microprocessor, programmable timing module, and priority encoders provide two significant improvements to the scanning system. The flexibility of the entire system has been greatly increased and the processing time has been significantly reduced. Future improvements can be added to the microprocessor based system, and electronics need not be designed from scratch. The programmable timing module frees the processor for other tasks and is itself so flexible that the scanning system could be converted into a measurement system. The encoders allow large amounts of data to be simplified in the order of microseconds to two easily handled 8 bit words. This processing time, which is crucial in any mobile robot, is of utmost importance.

The Mars Roving Vehicle and the Adaptive Suspension Vehicle are only two of a myriad of mobile robots yet to come. The ML/MD system discussed here has many more applications than just these two vehicles. As intelligent machines advance and become mobile, obstacle avoidance systems that are fast and accurate will be essential. These applications need to be investigated, and construction of this new system should begin as soon as possible. The new system will move the laser triangulation scheme back onto the edge of technology, and perhaps its value will be appreciated by more than just a few trying to prove its value now.

## PART 7

### REFERENCES

1. Goldstein, E. B., "Sensation and Perception." Wadsworth Publishing Company, California, 1980, Chap. 7.
2. Craig, J. and Yerazunis, S., "Elevation Scanning Laser Multi-Sensor Hazard Detection System Controller and Mirror/Mast Speed Control Components." Rensselaer Polytechnic Institute Technical Report MP-59, Troy, N.Y., August 1978.
3. Kennedy, W., "Control Electronics for a Multi-Laser/Multi-Detector Scanning System." Rensselaer Polytechnic Institute Technical Report MP-73, Troy, N.Y., August 1980.
4. McNeillis, T., "Evaluation of a Laser Triangulation Ranging System for Mobile Robots." Rensselaer Polytechnic Institute Technical Report MP-80, Troy, N.Y., August 1982.
5. General Scanning Inc., Series G Optical Scanners. General Scanning Inc., 1982.
6. Baker, C., "Laser Devices and Applications," IEEE Press, New York, 1973, p. 429.
7. Bademan, L., "Acousto-optical Deflectors." Isomet Corporation, Virginia, 1978.
8. Smith, H. M., Holographic Recording Materials. Topics in Applied Physics. 20, Chap. 1, 1977.
9. Kogelnik, H., Symposium on Modern Optics, Polytechnic Institute of Brooklyn, p. 605, March 1967.
10. Carlson, A. B., "Communication Systems - An Introduction to Signals and Noise in Electrical Communication." McGraw-Hill, New York, 1975., Chap. 5,6.
11. Case, S. K., "Multiple Exposure Holography in Volume Materials." The University of Michigan, p. 70, 1976.
12. Shankoff, T. A., "Phase Holograms in Dichromated Gelatin." Appl. Opt. 7, p. 2101, 1968.
13. Curran, R. K. and Shankoff, T. A., Appl. Opt. 9, p. 1651, 1971.

14. Fairchild, CCD Imaging and Signal Processing. Fairchild USA CCD Division, p. 122, 1981.
15. Taub, H. and Schilling D. "Digital Integrated Electronics." McGraw-Hill, New York, 1977, Chap. 12.